Supplementary Information

Impact of Isomeric Ligands on Molecular Stacking and Semiconducting Behavior in Square Planar Ni^{II} Complexes

Narayan Ch. Jana,[a] Mainak Das,[b] Paula Brandão,[c] Joaquín Ortega-Castro,[d] Antonio Frontera,[d] Partha Pratim Ray*,[b] and Anangamohan Panja,*,[a,e]

[a] *Department of Chemistry, Panskura Banamali College, Panskura RS, WB 721152, India.*

[b] *Department of Physics, Jadavpur University, Raja S. C. Mallick Road Jadavpur, Kolkata700 032, India. E-mail: parthapray@yahoo.com*

[c] *Department of Chemistry, CICECO-Aveiro Institute of Materials, University of Aveiro, 3810-193 Aveiro, Portugal*

[d] *Departament de Química, Universitat de les Illes Balears, Crta de valldemossa km 7.5, 07122 Palma de Mallorca (Baleares), SPAIN*

[e] *Department of Chemistry, Gokhale Memorial Girls' College, 1/1 Harish Mukherjee Road, Kolkata-700020. E-mail: ampanja@yahoo.co.in*

Characteristic spectra of ligands and complexes

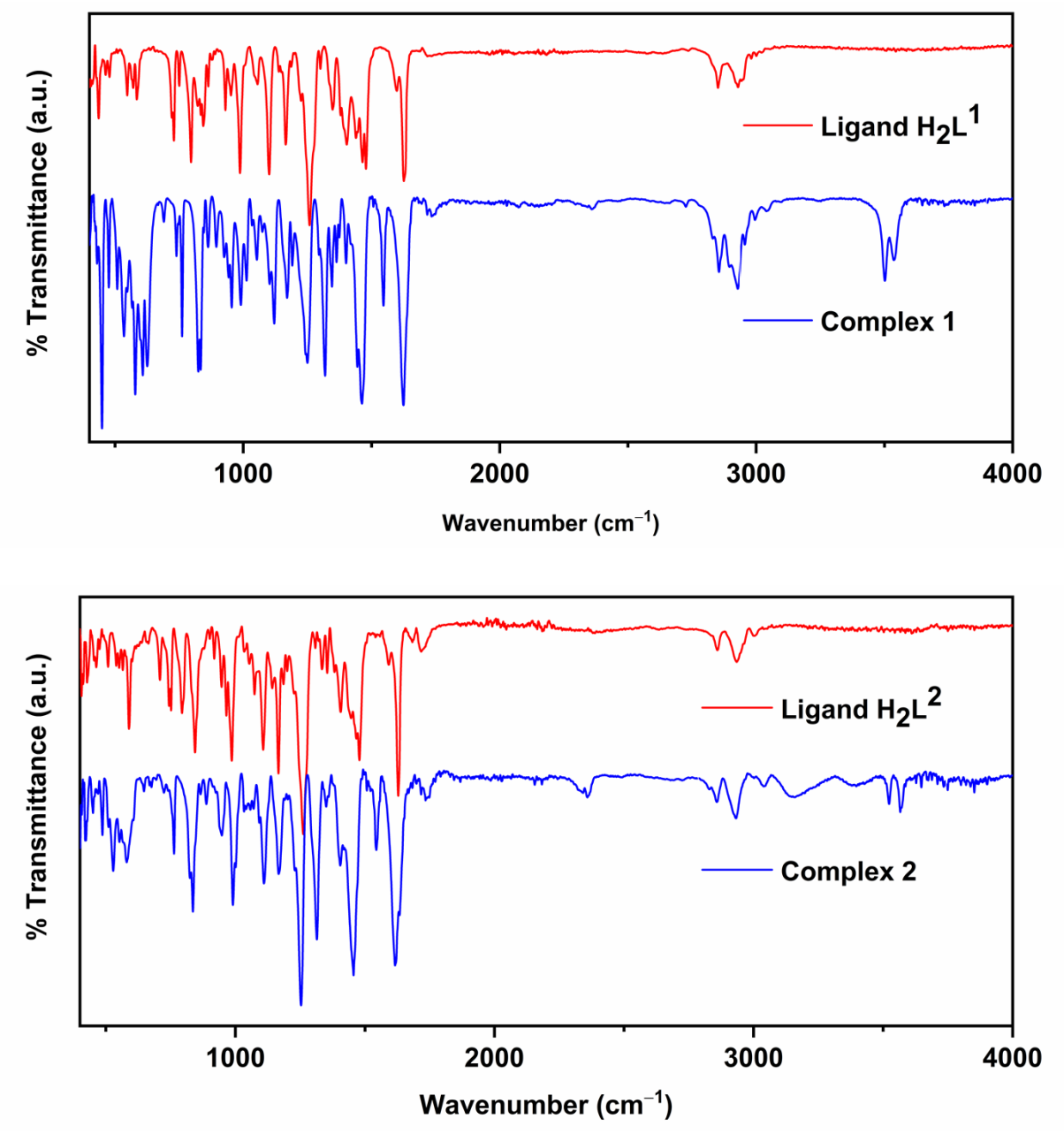

Figure S1: FT-TR spectra of the two ligands H_2L^1 and H_2L^2 and their corresponding complexes $[Ni(L^1)]\cdot H_2O$ (**1**) and $[Ni(L^2)]\cdot H_2O$ (**2**).

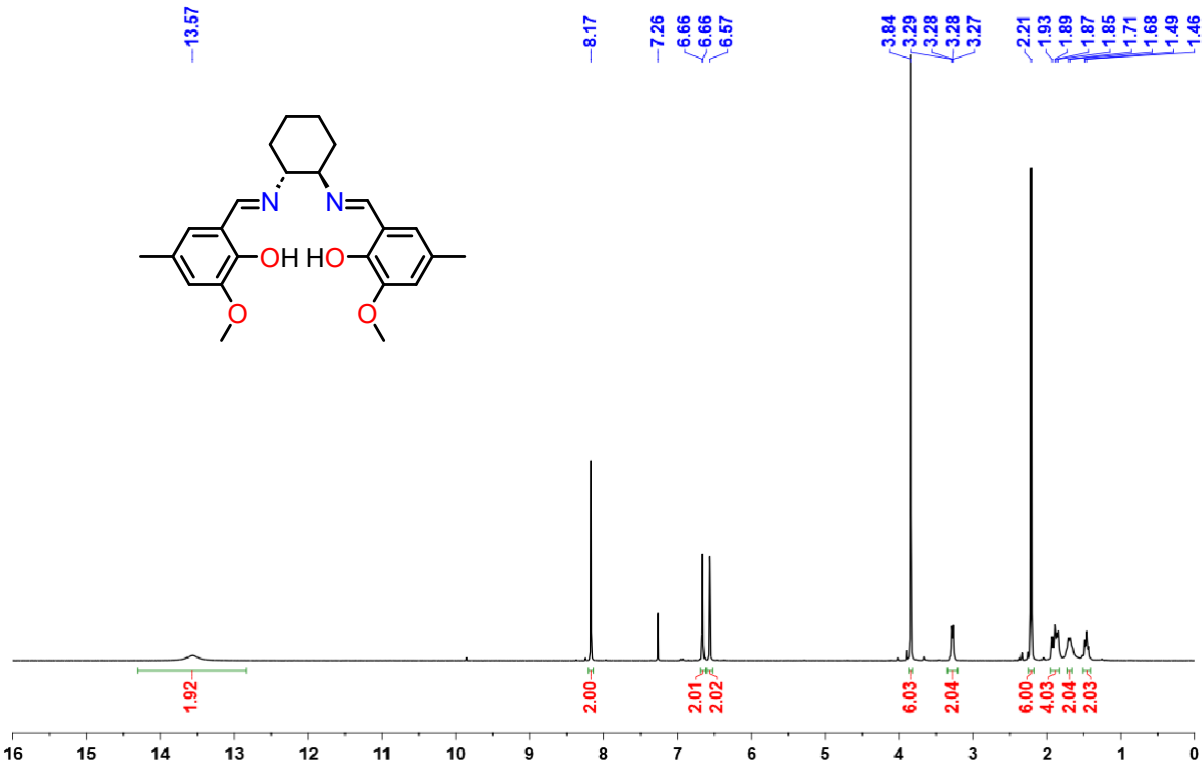

Figure S2: ^{1}H NMR of *trans-N,N'*-bis(3-methoxy-5-methylsalicylidene)-cyclohexane-1,2-diamine (H_2L^1) in $CDCl_3$ at room temperature.

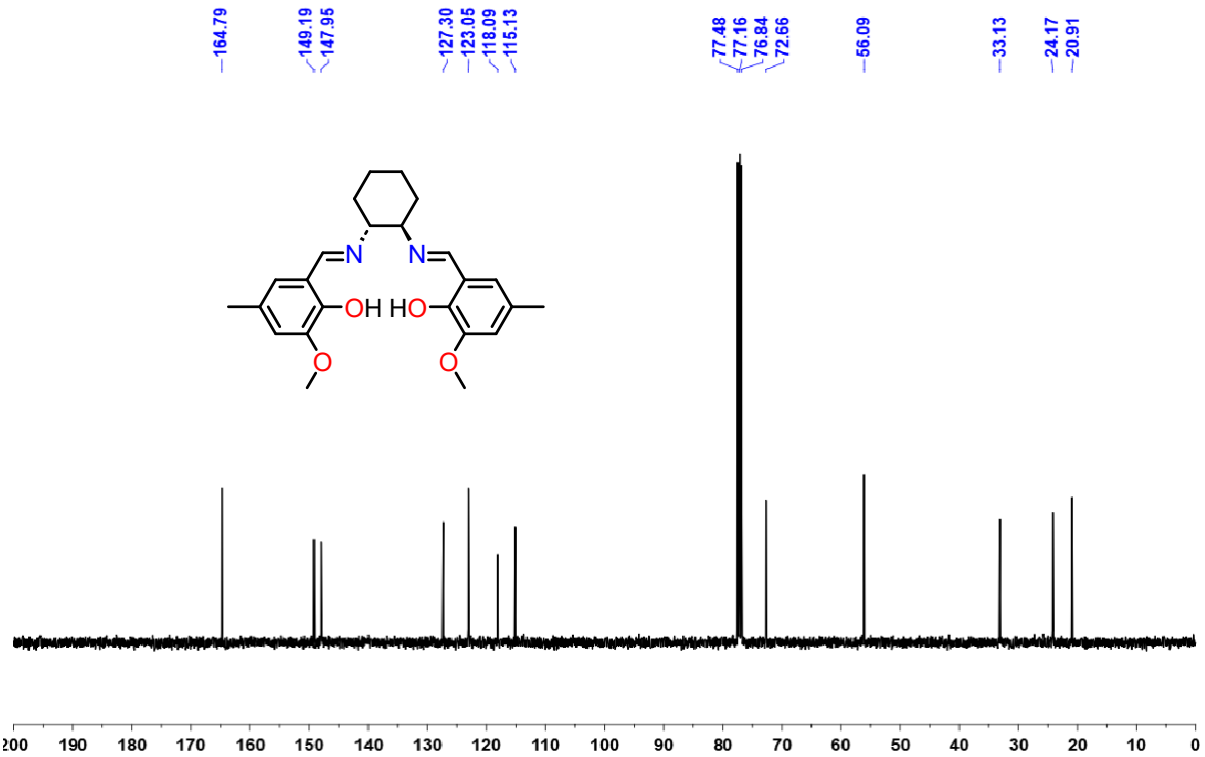

Figure S3: ^{13}C NMR of *trans-N,N'*-bis(3-methoxy-5-methylsalicylidene)-cyclohexane-1,2-diamine (H_2L^1) in $CDCl_3$ at room temperature.

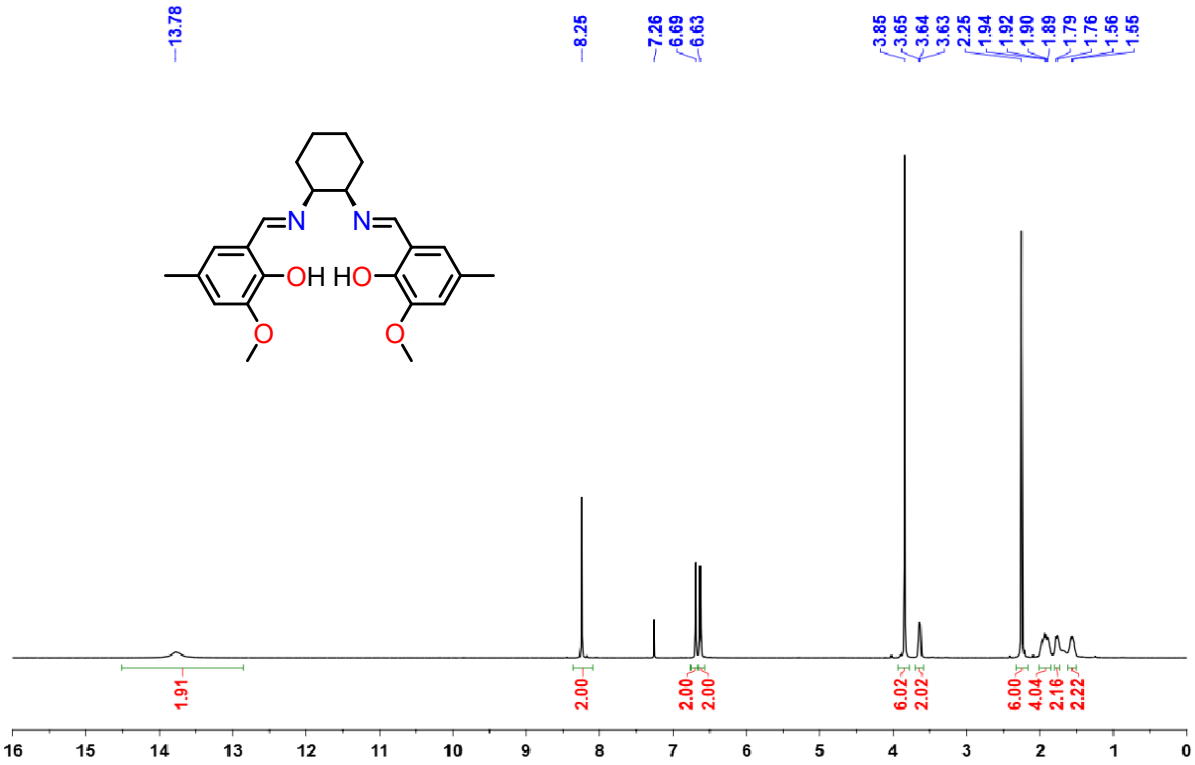

Figure S4: ^{1}H NMR of *cis-N,N'*-bis(3-methoxy-5-methylsalicylidene)-cyclohexane-1,2-diamine (**H_2L^1**) in $CDCl_3$ at room temperature.

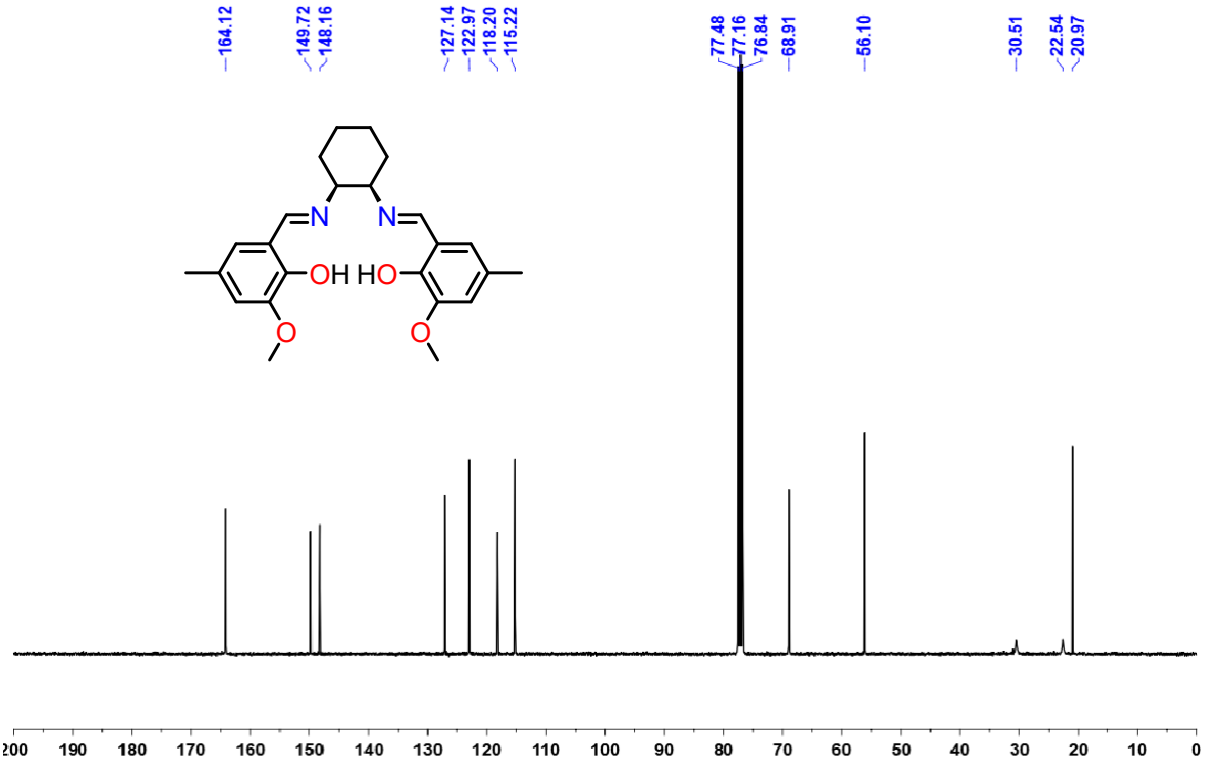

Figure S5: ^{13}C NMR of *cis-N,N'*-bis(3-methoxy-5-methylsalicylidene)-cyclohexane-1,2-diamine (H_2L^1) in $CDCl_3$ at room temperature.

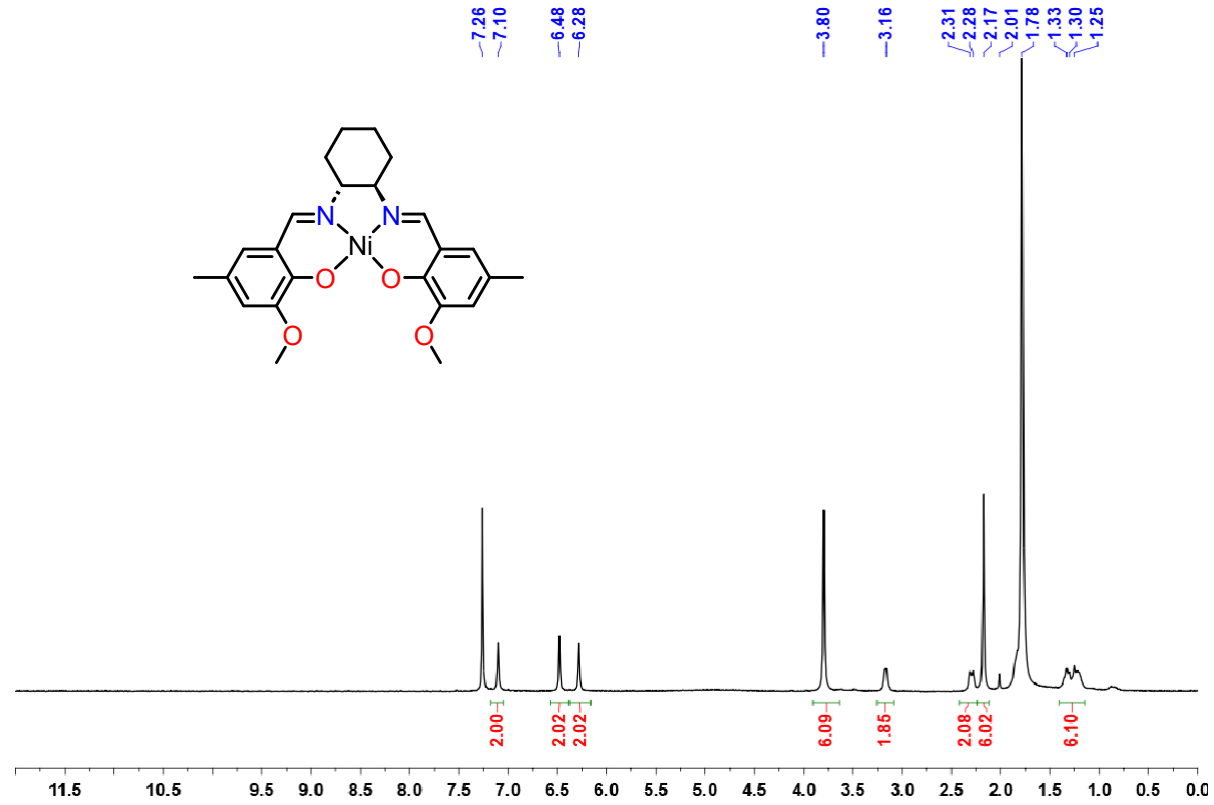

Figure S6: ^{1}H NMR of complex $[Ni(L^{1})]\cdot H_2O$ (**1**) in $CDCl_3$ at room temperature.

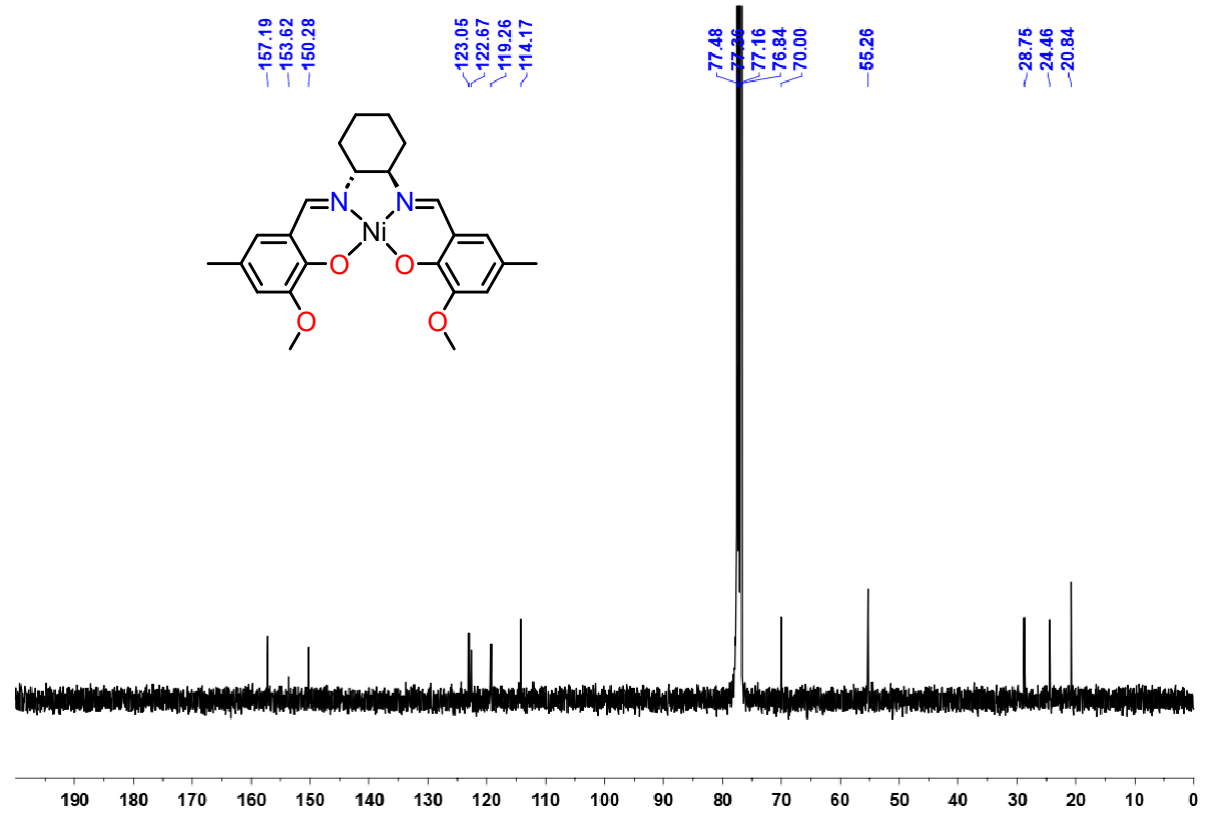

Figure S7: ^{13}C NMR of complex $[Ni(L^{1})]\cdot H_2O$ (**1**) in $CDCl_3$ at room temperature.

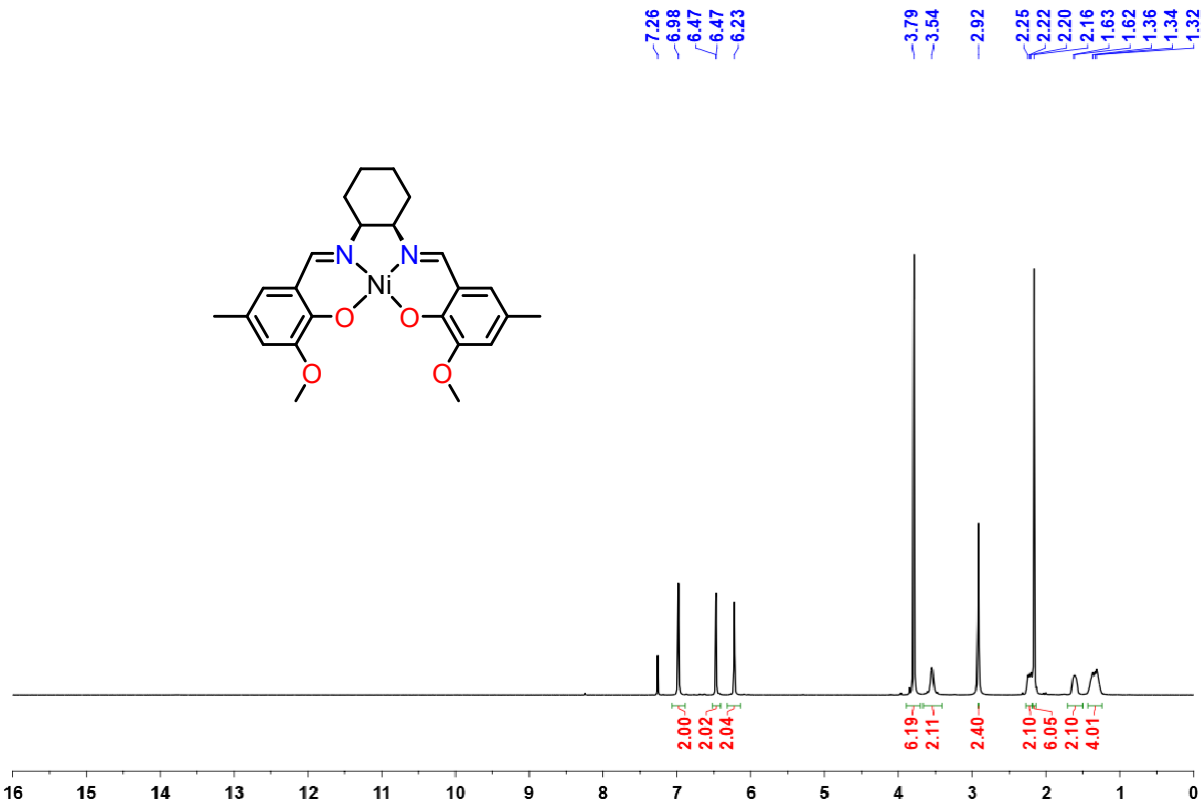

Figure S8: ^{1}H NMR of complex $[Ni(L^{2})]\cdot H_2O$ (**2**) in $CDCl_3$ at room temperature.

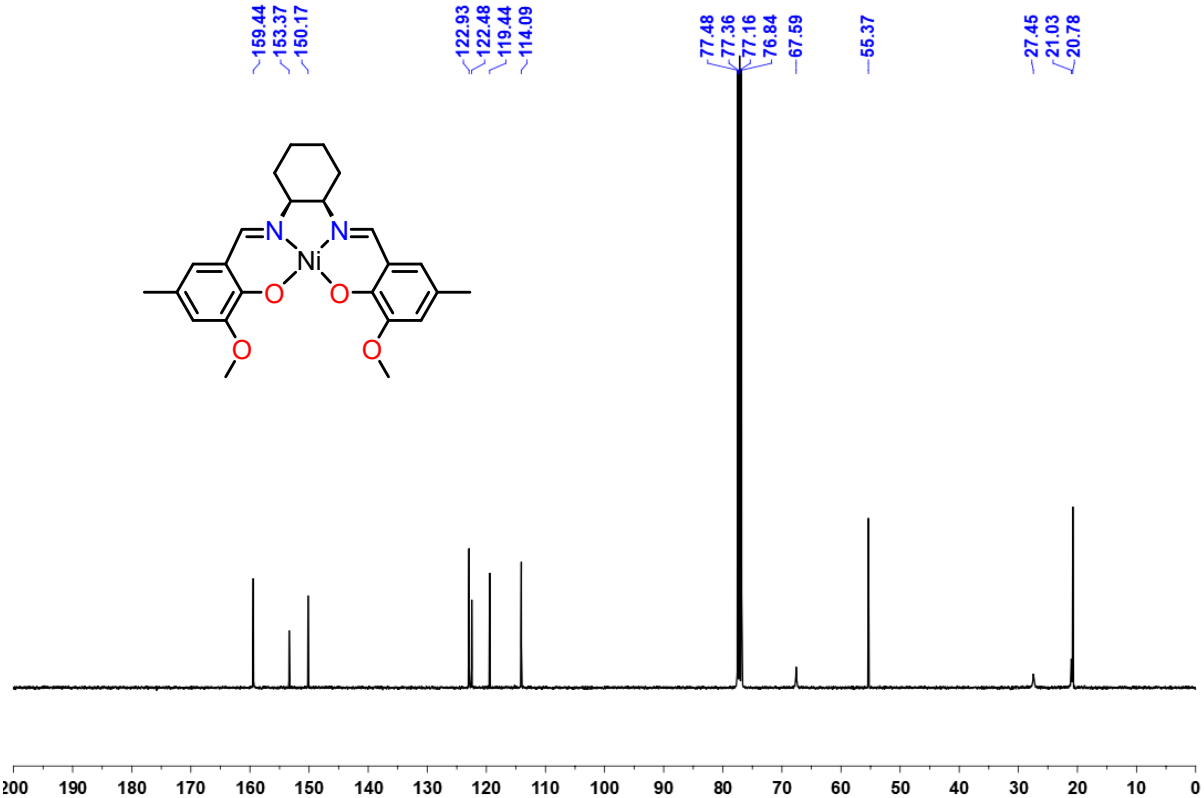

Figure S9: ^{13}C NMR of complex $[Ni(L^{2})]\cdot H_2O$ (**2**) in $CDCl_3$ at room temperature.

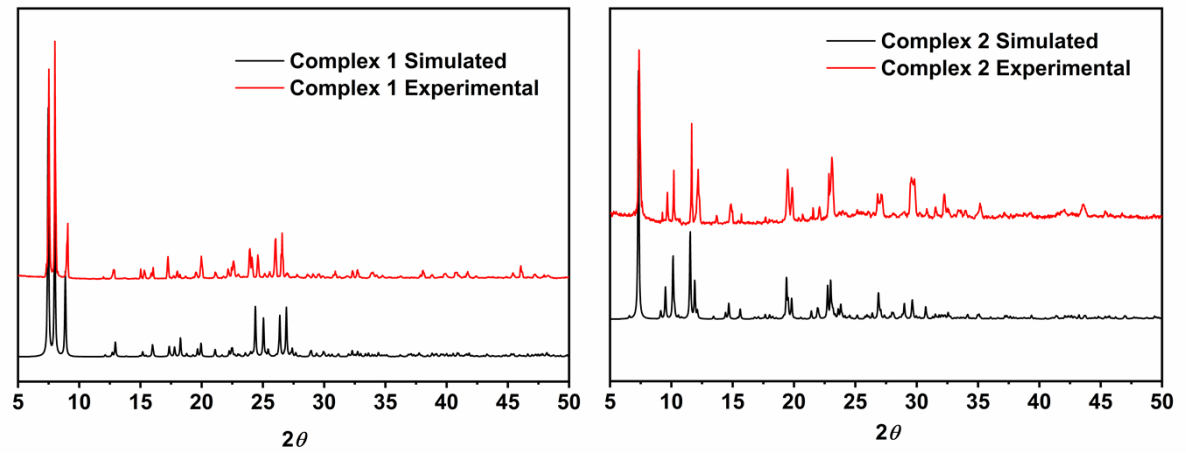

Figure S10. Experimental and simulated PXRD data for complex **1** and **2**.

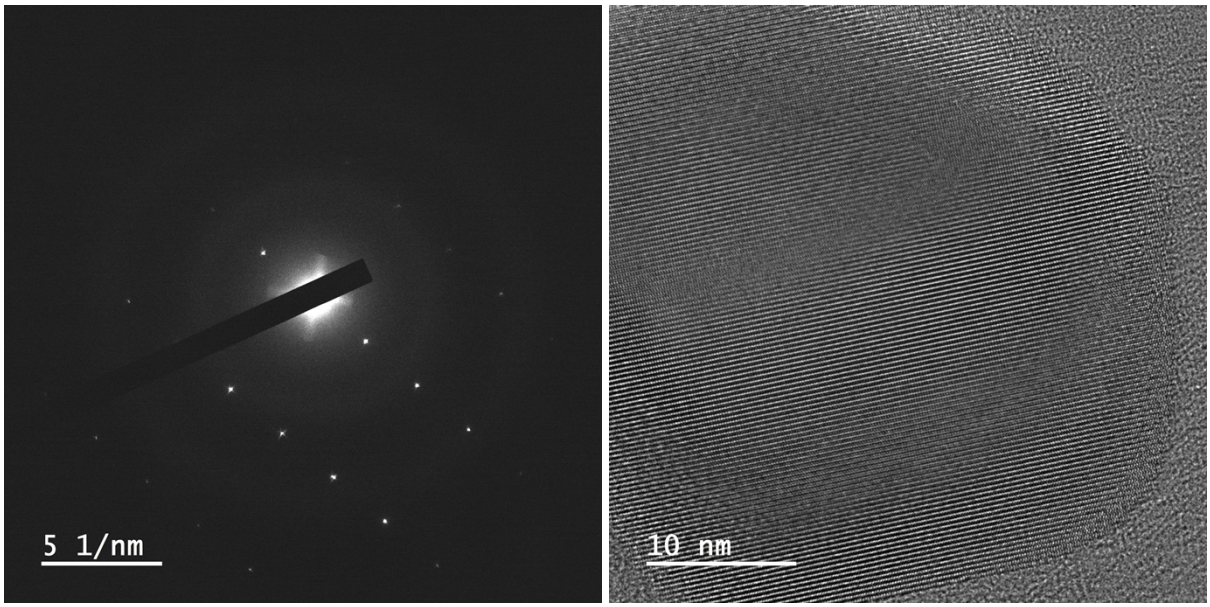

Figure S11. Selected area electron diffraction (SAED) pattern and HRTEM image obtained from a transmission electron microscope (TEM) for complex **2**.

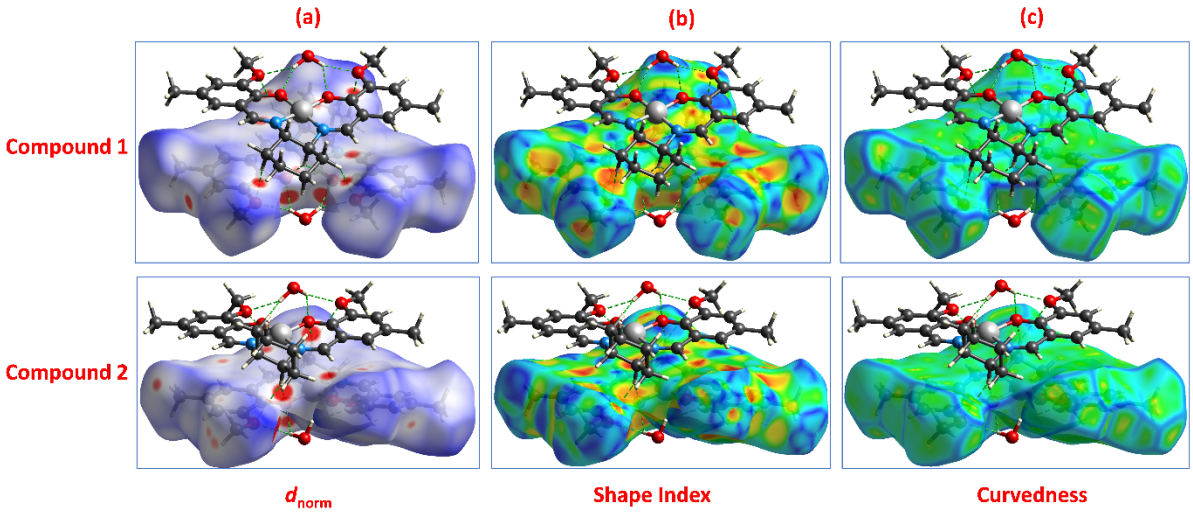

Figure S11. Hirshfeld surfaces of **1** and **2** stacked with dimeric: (a) 3D d_{norm} surface and (b) surface index and (c) curvedness.

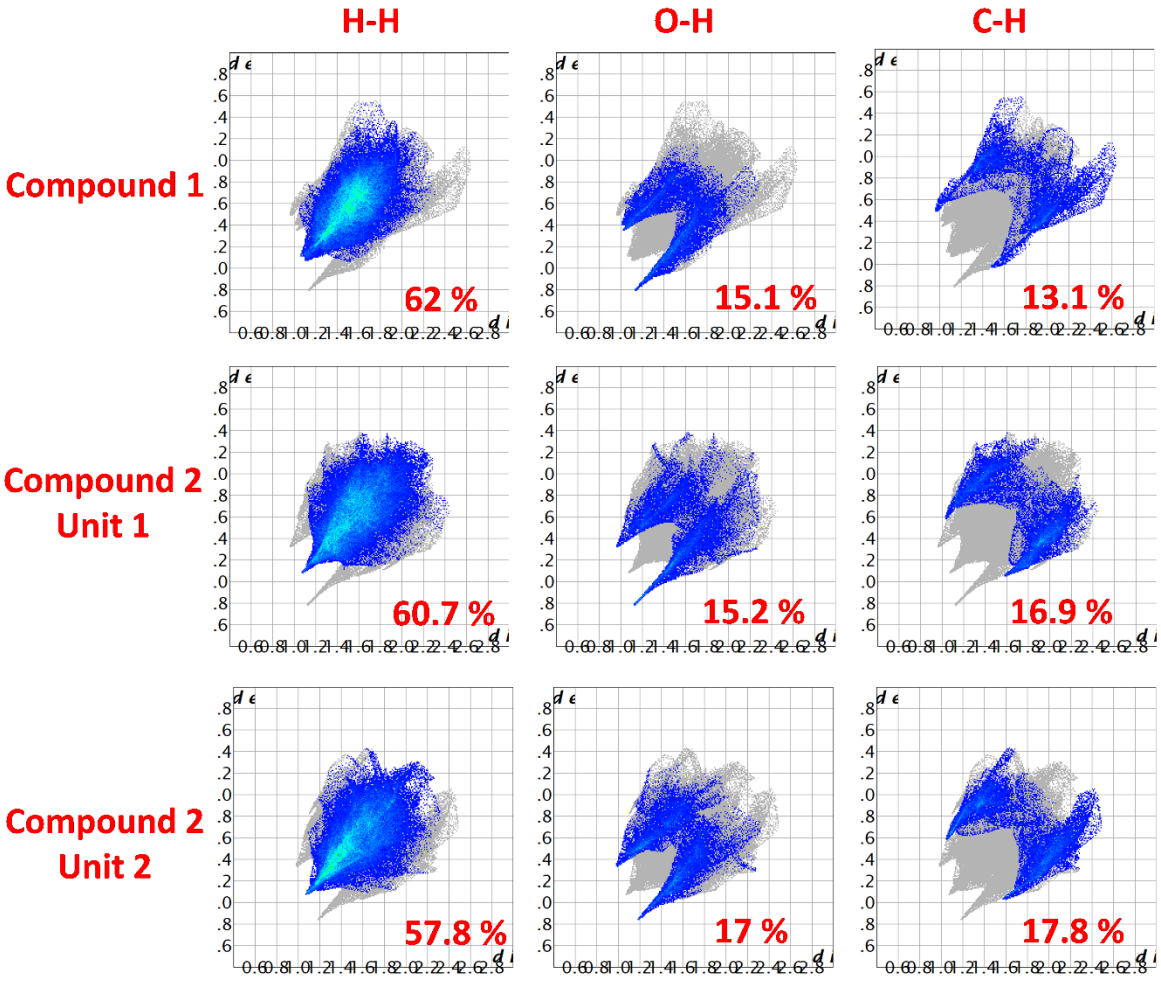

Figure S12. 2D fingerprint plots of the title compound **1** and **2** (crystallographic two different unit).

Table S1: Crystallographic parameters and refinement details for **1** and **2**.

	1	**2**
Empirical formula	$C_{24}H_{30}N_2O_5Ni$	$C_{24}H_{30}N_2O_5Ni$
Formula weight	485.209	485.21
Crystal system	monoclinic	monoclinic
Space group	$P2_1/n$	$P2_1/c$
a/Å	13.9644(12)	11.3463(7)
b/Å	7.8387(4)	16.1675(9)
c/Å	19.9931(14)	24.1553(15)
α/°	90	90
β/°	94.284(4)	91.281(2)
γ/°	90	90
Volume/Å^3	2182.4(3)	4430.0(5)
Z	4	8
ρ_{calc}g/cm^3	1.477	1.455
μ/mm^{-1}	0.929	0.915
F(000)	1026.1	2048.0
2Θ range for data collection/°	5.58 to 61.1	4.21 to 54.33
Reflections collected	54758	98144
Independent reflections	6664 [R_{int} = 0.0671, R_{sigma} = 0.0354]	9807 [R_{int} = 0.0497, R_{sigma} = 0.0242]
Data/restraints/parameters	6664/0/296	9807/0/596
Goodness-of-fit on F^2	1.039	1.067
Final R indexes [I>=2σ (I)]	R_1 = 0.0320, wR_2 = 0.0767	R_1 = 0.0394, wR_2 = 0.0937
Final R indexes [all data]	R_1 = 0.0394, wR_2 = 0.0808	R_1 = 0.0555, wR_2 = 0.1019
Largest diff. peak/hole / e Å^{-3}	0.80/-0.39	0.70/-0.54

Table S2: Important bond distances and bond angles in complex **1** and **2**.

Bond	Length (Å)			Bond	Angle (°)		
	1	**2**			**1**	**2**	
		A	**B**			A	B
Ni–O1	1.8634(10)	1.8470(16)	1.8477(17)	O1–Ni1–O3	85.66(4)	85.32(7)	85.02(7)
Ni–O3	1.8651(10)	1.8556(15)	1.8514(16)	O1–Ni1–N2	174.04(5)	172.17(8)	174.45(8)
Ni–N1	1.8584(11)	1.8578(19)	1.860(2)	N1–Ni1–O1	94.57(5)	95.29(8)	95.12(8)
Ni–N3	1.8636(12)	1.8460(19)	1.852(2)	N1–Ni1–O3	175.50(5)	172.69(8)	172.72(8)
				N2–Ni1–O3	94.32(5)	94.54(7)	94.18(8)
				N1–Ni1–N2	85.93(5)	85.85(8)	86.37(9)

Device Fabrication and Characterization:

The fabrication of the Schottky device was made by following procedures. At first, Indium Tin Oxide (ITO) coated glass substrate was cleaned by acetone, distilled water and isopropanol

repeatedly and sequentially in ultra-sonication bath for 30 min. At the same time a well dispersed solution of the AM-089 and AM-652 in N N-dimethyl formamide (DMF) medium was prepared and spin coated onto the pre-cleaned ITO coated glass at 800 rpm for 2 min with the help of SCU 2700 spin coating unit. This spin coating step was repeated for 3 times. After drying in vacuum, the film thickness was measured as 1 μm by surface profiler. Aluminum (Al) electrodes were deposited onto the film by a Vacuum Coating Unit 12A4D of HINDHIVAC under a pressure of 10^{-6} Torr. The area of the Al electrodes was maintained as 7.065×10^{-6} m^2 by the shadow mask. The current-voltage measurements of the fabricated device with AM-089 and AM-652 were carried out by a Keithley 2635B source meter interfaced with PC by two-probe technique under ambient condition in the voltage range -1V to +1V at room temperature.

Electrical Characterization:

The Thermionic Emission (TE) theory is adopted to get more insights of the charge transport mechanism in the devices.[1] The current of a diode can be expressed as the following equations according to TE theory.[2]

$$I = I_0 \exp\left(\frac{qV}{\eta kT}\right)\left[1 - \exp\left(-\frac{qV}{\eta kT}\right)\right] \quad \ldots\ldots(S1)$$

Where,

$$I_0 = AA^*T^2 \exp\left(-\frac{q\phi_B}{kT}\right) \quad \ldots\ldots(S2)$$

$$\phi_B = \frac{kT}{q} \ln\left(\frac{AA^*T^2}{I_0}\right) \quad \ldots\ldots\ldots(S3)$$

Where, I_0 indicates the saturation current, q represents the electronic charge, k is the Boltzmann constant, T is the temperature in Kelvin, V is the forward bias voltage, η is the ideality factor, ϕ_B is the effective barrier height at zero bias, A is the diode area (7.065×10^{-6} m^2), A^* is the effective Richardson constant (1.20×10^6 $Am^{-2}K^{-2}$). From Cheung, the forward bias I-V characteristics in term of series resistance can be expressed as.[3]

$$I = I_0 \exp\left[\frac{q(V - IR_S)}{\eta kT}\right] \quad \ldots\ldots. (S4)$$

Where, the IR_S term represents the voltage drop across series resistance of device. In this circumstance, the values of the series resistance can be determined from following functions using equation (S5 & S6).[4]

According to Cheung's model:

$$\frac{dV}{dln(I)} = \left(\frac{\eta kT}{q}\right) + R_S I \qquad \text{……. (S5)}$$

$$H(I) = R_S I + \eta\phi_B \qquad \text{……(S6)}$$

and H(J) can be expressed as:

$$H(I) = V - \left(\frac{\eta kT}{q}\right) ln\left(\frac{I}{AA^* T^2}\right) \qquad \text{……. (S7)}$$

REFERENCES

1. E. H. Rhoderick and R. H. Williams, Metal-Semiconductor Contacts, Clarendon Press, Oxford, 2nd edn, 1988.

2. S. M. Sze, Physics of Semiconductor Devices, Wiley, New York., 1981.

3. S. Sil, R. Jana, A. Biswas, D. Das, A. Dey, J. Datta, D. Sanyal, and P. P. Ray, *IEEE Trans. Electron Devices* 2020, **67**, 2082– 2087.

4. S. Mahato, A. Mondal, M. Das, M. Joshi, P. P. Ray, A. Roy Choudhury, C. M. Reddy, and B. Biswas, *Dalton. Trans.* 2022, **51**, 1561– 1570.